LIGHTWEIGHT METAL CELLULAR STRUCTURES VIA INDIRECT 3D PRINTING AND CASTING

Nicholas A. Meisel, Christopher B. Williams, Alan Druschitz
Design, Research, and Education for Additive Manufacturing Systems Laboratory
Department of Mechanical Engineering
Virginia Polytechnic Institute and State University
REVIEWED, Accepted August 16, 2012

ABSTRACT

Cellular materials offer high strength accompanied by low-density and can offer high stiffness, good impact-absorption, and thermal and acoustic insulation. In this paper, the authors describe their progress towards exploring the use of metal casting into 3D printed sand molds for creating cellular materials and sandwich panels. The use of 3D printing allows for the fabrication of sand molds without the need for a pattern, and thus enables the creation of cellular structures with designed mesostructure from a bevy of metal alloys. The quality-of-fill results for several cast aluminum cellular parts of varying geometry are presented in this paper, along with a discussion of overall truss diameter variation.

Keywords: Indirect 3D Printing, Cellular Structures, Metal Casting

1. MOTIVATION

As military vehicles and infrastructure face ever increasingly lethal threats, there is continued interest for lightweight ballistic armor that will improve vehicle performance and safety and also decrease vehicle transportation costs. Cellular materials (metallic bodies with interdispersed voids) are a promising class of structures for addressing this need. Cellular materials offer high strength accompanied by low-density [1] and can offer high stiffness, good impact-absorption, and thermal and acoustic insulation [2].

Recent cellular material research has focused in designing the mesoscopic topology (the geometric arrangement of the solid phases and voids within a material or product of the size range of 0.1 to 10 mm) in order to effectively support and improve multiple design objectives [3-5]. Example applications of designed cellular mesostructure include a jet engine combustor liner that has sufficient strength to withstand extreme pressures and stresses from thermal expansion while still maintaining open cells that allow for active cooling via forced convection (Figure 1a) [6] and a lightweight blast resistant panel that efficiently absorbs impact from large impulse forces (Figure 1b) [7].

Due to the complex internal geometry, manufacturing a component with cellular mesostructure is impossible with traditional subtractive machining. As such, researchers have looked to advanced manufacturing technologies to produce this unique class of materials.

(a) combustor liner [10] (b) blast resistant panel [12]

Figure 1. Examples of Cellular Materials with Designed Mesostructure

1.1. Traditional Cellular Material Manufacturing

Stochastic metal foaming processes feature forming gas in liquid metal (Alporas, Hydro/Alcan/Combal, Gasar/Lotus processes), or by mixing metal powders with a blowing agent which is then compacted and melted (Alulight/Foaminal techniques) [1]. While these processes result in structures with cells of random shape, morphology, and distribution [8], they "place material in locations where it contributes little to material properties (other than density)" [4]. The largest limitation of stochastic cellular structures is the complete lack of control that a designer has over the topology of the mesostructure; the techniques do not provide repeatable, or even predictable, results [2]. Furthermore, these techniques limit a designer in the types of macrostructure that can be made.

Ordered cellular materials are characterized by a periodic unit cell or by a repeating structure throughout the part. Compared to stochastic materials, ordered structures have superior mechanical properties, including energy absorption, strength, and stiffness [9]. Ordered cellular materials have been made by stamping or crimping thin sheets of metal into a corrugated shape and then joining them to create periodic structures [10]. Alternatively, they have been created by joining and bonding slotted metal sheets [11], extrusion and electrodischarge machining [12], and weaving and brazing metal filaments to form a periodic textile [13,14]. Although these fabrication techniques offer repeatable part quality, they limit the macrostructure of resulting parts to planar geometries [15], and constrain a designer to the use of a specific homogeneous mesostructure throughout a part.

1.2. Fabricating Cellular Materials with Designed Mesostructure via Additive Manufacturing

While stochastic and ordered cellular material manufacturing techniques are capable of producing light-weight and strong cellular materials, process limitations prevent a designer from tailoring part mesostructure for specific design intent(s) [4]. To address these limitations, researchers have turned to Additive Manufacturing (AM) as a means of fabricating these materials. The layer-by-layer nature of AM processes enable the creation of complex geometries that cannot be fabricated by any other means. These processes thus provide a designer the freedom to tailor part geometry for specific design intent(s).

Direct-metal AM processes, which selectively scan an energy source, such as a laser or electron beam spot over a metal powder bed, are capable of fabricating fully-dense metal artifacts without the need for additional post-processing. Selective Laser Melting [16, 17], Electron Beam Melting [18, 19], and Direct-Metal Laser Sintering [20] have all been employed in research targeted towards fabricating cellular materials. While these processes have been successfully used to fabricate parts with cellular geometries, their ability to make parts of designed mesostructure is limited by inherent process constraints [21]. Specifically, direct-metal AM processes have a limited set of working materials; for example, aluminum alloys are challenging to process due to high thermal conductivity and high optical reflectivity. Fabricated parts also suffer from residual stresses [22, 23] and/or require the use of support structures or anchors when fabricating large parts with significant overhanging geometries [24]. The required use of support scaffolds (which must be manually removed later) is especially limiting when trying to create large cellular geometries, as they would be difficult to remove from the interior cells. In addition, these processes are relatively expensive and have a low throughput due to their use of a 1D energy patterning mechanism (i.e., a laser). For these reasons, it can be argued that direct-metal AM techniques are not capable of fabricating cellular structures of a sufficient scale for vehicle armor applications.

1.3. Indirect Fabrication of Cellular Materials via AM and Metal Casting

Given the existing limitations of cellular material manufacturing processes, and the design constraints that they impose on the resultant cellular parts, the goal of this research is to develop a manufacturing process capable of producing metallic cellular structures with designed mesostructure. To achieve this goal, the authors look to a hybrid manufacturing process that combines the geometric freedoms offered by AM with the material qualities offered by metal casting. Specifically, the authors are investigating a process chain wherein Indirect 3D Printing (3DP) is used to directly fabricate sand molds for metal casting lightweight cellular structures.

A review of previous efforts in using metal casting to fabricate cellular materials is offered in Section 2. An overview of the hybrid 3DP/casting process chain is presented in Section 3. Qualitative pour analysis of components fabricated by the hybrid process is presented in Section 4, along with an investigation into truss diameter variation . Closure and future work is offered in Section 5.

2. FABRICATING CELLULAR MATERIALS VIA METAL CASTING

In the early 2000's Jamcorp Inc. explored the use of sand casting to process Lattice Block Materials (LBM) [25]. The company used specially made preforms to create trussed structures. Due to the difficulty in fabricating complex patterns for creating the sand molds, the resulting parts had a planar macrostructure, and a fixed (pyramidal) mesostructure. To alleviate these geometric constraints, the company also investigated investment casting of LBMs. However, the resulting components suffered from porosity due to the inability of the fluid to access all parts of the truss structure [26, 27]. As such, cellular materials created by casting must have trusses of a certain diameter and all cells must be interconnected.

2.1. AM & Metal Casting Hybrid Processes

To address the geometric constraints imposed by traditional casting and pattern fabrication, a few hybrid manufacturing processes have been proposed. In these processes, AM techniques are used to fabricate polymer patterns, which are then used to create molds for metal casting. For example, in research conducted by Hattiangadi and Bandyopadhyay, Filament Fabrication (FFF) is used to produce a geometrically complex wax pattern, which is then coated in ceramic, burned away, and cast with metal [28]. Similarly, Chiras and coauthors used AM to create truss structure patterns for investment casting process with a high fluidity Be-Cu alloy, Figure 2 [29]. In addition to FFF, MultiJet Modeling has been used to fabricate wax patterns for a lost wax casting technique to fabricate complex heat exchanger designs [30].

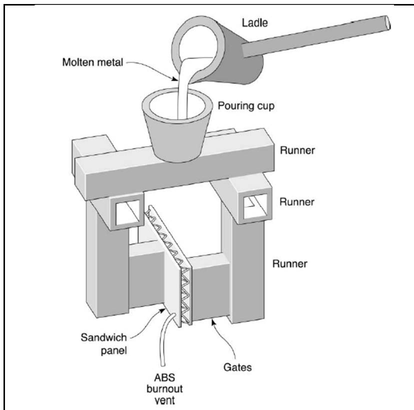

Figure 2. Investment Casting of Lattice Block Material from ABS Pattern (Chiras 2002)

2.2. Patternless Sand Casting via Indirect 3D Printing

In this work, the authors look to Indirect 3DP as a means of directly fabricating a sand mold for casting cellular materials. Indirect 3DP is an AM technology that creates artifacts through the deposition of binder into a powder bed of raw material. Once a layer has been printed, the powder feed piston raises, the build piston lowers, and a counter-rotating roller spreads a new layer of powder on top of the previous layer. The subsequent layer is then printed and is stitched to the previous layer by the jetted binder. A schematic of the indirect 3D printing process can be seen in Figure 3.

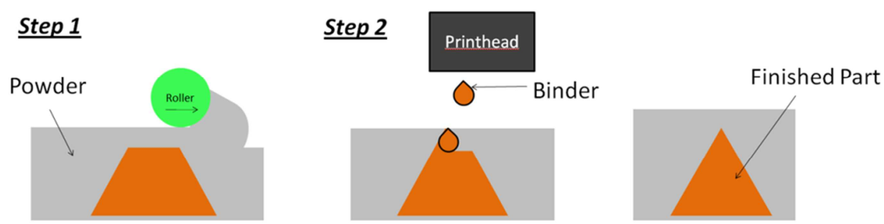

Figure 3. Indirect 3D Printing Schematic

By selectively printing binder into a bed of foundry sand layer-by-layer, Indirect 3DP can be used to directly fabricate molds for metal casting. As with all AM processes, 3DP offers tremendous design freedom for altering mold geometry; with this technology, molds can be fabricated with integrated gating systems, embedded cores, and without the need for a pattern. The technology is commercially offered by ZCorp's ZCast material [31], ExOne's S-Max and S-Print machines [32], and VoxelJet [33]. Direct digital fabrication of sand molds for casting eliminates the costs associated with pattern tooling and is thus ideal for low volume production [34, 35].

Existing research on the use of Indirect 3DP for metal casting has been primarily focused in casting case studies and studies of resultant material properties [36-40]. The technology has been shown to be effective in obtaining cast prototypes with dimensional tolerances that are consistent with metal casting processes [41]. However, there does not exist any literature pertaining to the use of this technology to fabricate complex geometries. Studies in which part complexity is explored are limited to case studies in which existing products are cast with redesigned mold and core shapes [42, 43].

Indirect 3DP is a suitable AM process for the fabrication of complex cellular geometries since there is no need for a separate support material that must be removed in post-processing [44]. Overhanging structures are supported by the unbound powder within the powder-bed during fabrication. Once printing is complete, the unbound powder is removed from the printed part using compressed air. The ability to fabricate complex sand molds without patterns is especially beneficial for fabricating cellular materials – a cellular pattern could not be removed from a sand mold using traditional sand casting techniques. In addition, Indirect 3DP is inherently scalable – the use of 2D material deposition (i.e., large inkjet printheads) result in relatively short build times when compared to powder-bed fusion direct-metal processes.

3. INDIRECT 3D PRINTING OF SAND CASTING MOLDS FOR CELLULAR MATERIAL FABRICATION

The proposed procedure for creating cast metal parts with a designed mesostructure via indirect 3D printing follows six distinct steps:

1. Design the desired mesostructure as a solid model in CAD and perform a Boolean subtraction of the mesostructure from the desired overall geometric shape.
2. Print the mold utilizing the necessary material-dependent printing parameters.
3. Clean the printed mold, ensuring that all channels are clear, followed by heat treatment of the mold.
4. Create exterior mold to surround printed mold, incorporating necessary casting aspects (e.g. gates, runners, downsprue).
5. Cast desired metal into mold.
6. Clean the metal part of remaining mold sand and flash, followed by heat treatment to ensure adequate mechanical properties.

With this process, the authors have been able to create a wide variety of cellular geometries from a range of castable metals.

3.1. Digital Mold Design

The indirect 3D printing process allows for simple creation of complex mold structures from a 3D solid model. For this work, the complex mold is designed using netfabb's Selective Space Structures (SSS) software [45]. To create the final mold, the designed truss structure is Boolean subtracted from a prismatic solid. An example of this process is shown in Figure 4. A repeating octet truss structure is designed using netfabb SSS; the corresponding mold is created via a Boolean subtraction from a 2-inch solid cube. The Boolean subtraction need not be performed using a cube, as other shapes, such as a hemisphere, will work as well (as shown in Figure 7 in Section 4.1).

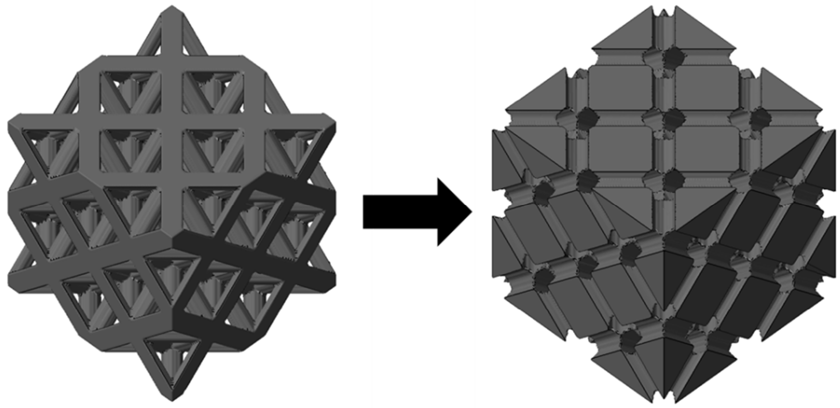

Figure 4. Desired Final Shape and Necessary Printed Mold (After Boolean Subtraction)

3.2. Mold Creation

With the digital creation of the mold completed, and exported to .STL format, the file is imported into the 3DP's accompanying software (ZPrint), where it is oriented, scaled, and positioned. As with other powder-bed processes (with direct-metal being the exception), indirect 3D printing allows for the build volume to be completely filled with parts, thus further increasing the throughput of the process, and further improving the time-to-cast compared with traditional casting mold creation.

In this work, ZCorp's Spectrum 510 is used for printing of the molds. The authors have investigated two powder materials: ViriCast 170LE (Viridis3D LLC) and ZCast 501 (ZCorp). ZCast 501 is a mixture of foundry sand, plaster, and additives which allows for the casting of low temperature (non-ferrous) metals such as aluminum, zinc, and magnesium [31]. The ViriCast powder has the added advantage of being capable of casting ferrous metals, such as steel, allowing for greater variety in the final casting product. The printing parameters for both the ViriCast 170LE and ZCast 501 molds are summarized in Table 1.

Table 1. Print Settings for ZCast 501 and ViriCast 170LE Powders

	ZCast 501	**ViriCast 170LE**
Layer Thickness	0.005 inches	0.004 inches
Saturation Level (Shell)	94%	65%
Saturation Level (Core)	49%	88%
Binder/Volume Ratio (Shell)	0.204517	0.179066
Binder/Volume Ratio (Core)	0.0530748	0.121214
Bleed Compensation (X)	N/A	0.0056 inches
Bleed Compensation (Y)	N/A	0.0051 inches
Bleed Compensation (Z)	N/A	0.0039 inches

Once printed, parts remained in the powder bed for 60 minutes to allow the jetted binder to fully cure. They were then removed and brushed of excess powder. Because of the complex truss structure involved in each mold, additional detailed cleaning was required, where compressed air and a stiff metal wire were used to ensure that each through-channel was clear of any excess powder. After cleaning, each part was heat treated (250 °F for 2.5 hours, followed by 1.75 hours at 450 °F) to ensure that no moisture remained in the mold, and thus making them suitable for metal pouring. An example of a final printed rectangular mold can be seen in Figure 5.

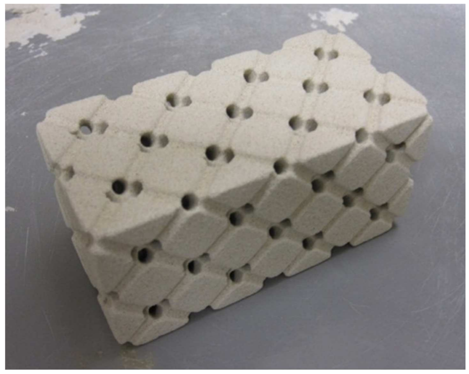

Figure 5. Final Printed Mold of Rectangular Geometry

With the printed mold prepared, it is necessary to create an outer mold, consisting of a downsprue, gates, and runners, to enable the filling of the printed mold. These mold elements direct the molten metal flow as desired, i.e. filling the printed mold from the bottom to the top. The design of the outer mold also allows for additional characteristics to be added to the desired mesostructure; in these examples, a gap between the outer mold and the printed mold creates a solid plate both above and below the designed mesostructure. This outer mold can be either 3D printed, or can be made from traditional foundry lake sand that is typically used for mold creation. The printed cellular mold is encased inside the prepared cope and drag sections, as shown in Figure 6.

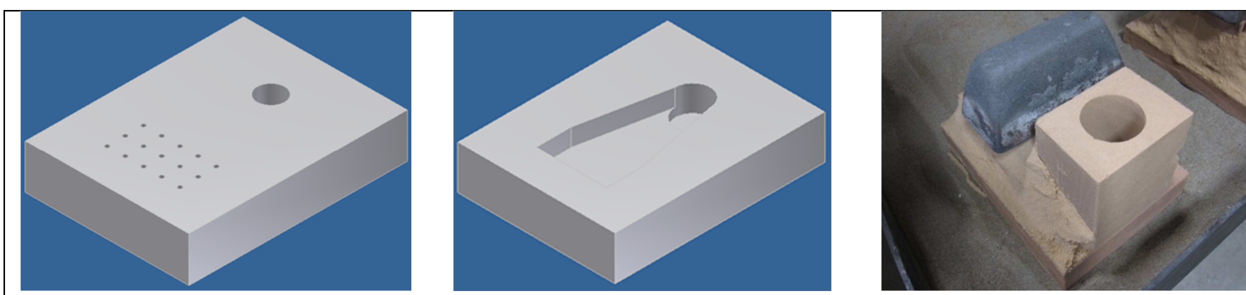

(a) (b) (c)

Figure 6. Cope (a) and Drag (b) CAD Models with Hand Created Final Outer Mold (c)

3.3. Metal Part Creation

Castings were poured in A356 alloy, a common aluminum alloy used in safety critical automotive applications due to its good combination of mechanical properties and castability. A356 ingot was melted in a SiC crucible using an electrical resistance furnace. The temperature of the metal in the furnace was limited to a maximum of about 760 °C (1400 °F); molten metal temperature was measured using an immersion thermocouple. Approximately 2 minutes before pouring, TiBor (Al-5wt%Ti-1wt%B) was added for grain refinement and Al-10wt%Sr was added for silicon modification. The castings were poured along with a chilled spectrometer sample for determining chemistry. The actual pouring temperature was not measured but would be expected to be ~10-20 °C lower than the temperature in the furnace (actual pouring temperature: ~740-750 °C, ~1365-1380 °F).

At first, the gating system for metal pouring was designed to fill the mold as quickly as possible but, for subsequent pours, the gating system has been modified to increase the pour time and slow the metal flow (e.g. though the use of a ceramic foam filter). Castings were relatively easy to clean. Sufficient heat was available to burn-out enough of the binder such that only light pressure on a pointed instrument was enough to break the mold apart. No sand burn-on or metal penetration into the mold was noted. Sand or shot blasting were not necessary to produce a clean casting.

The cleaned castings were given a standard T6 heat treatment (solution treatment followed by artificial aging) to produce a good combination of strength and ductility. The castings were heated to 540 °C (1005°F) in an air circulating furnace and held for about 11 hours at temperature to spheroidize the silicon particles and put the strengthening elements into solid solution. At the end of the high temperature cycle, the castings were removed from the furnace and quenched in a bucket of room temperature water. Next, the castings were artificial aged at 154 °C (310 °F) for 5 hours. During heat treatment, the actual casting temperature was measured using a chromel-alumel thermocouple attached to the casting.

4. RESULTS

The proposed process was used to create lightweight metal parts of various geometric shapes, each with an octet-truss based internal structure. While the final parts are not necessarily of uniform quality, several observations can be made from the results regarding the quality of the part fill and the mechanical properties of the parts.

4.1. Quality of Part Fill

As discussed previously, this methodology allows for the creation of parts of designed mesostructure that adhere to different shape profiles. Three distinct shapes were investigated, a 2” x 2” x 2” cube, a 2” x 2” x 4” rectangular prism, and a hemisphere with a radius of 1.5”. While the molds for all three shapes were printed successfully, the quality of the final cast part appears to be dependent, in part, on the dimensions and shape of the desired shape. Representative images of each cast shape can be seen in Figure 7.

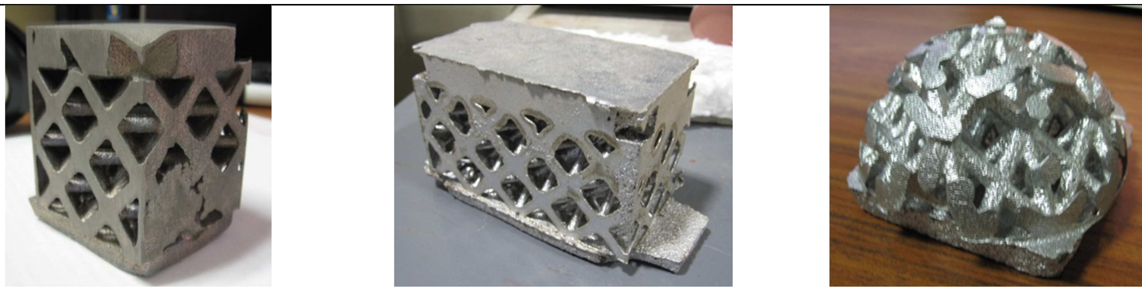

(a) (b) (c)

Figure 7. Final Cast Parts: (a) Cube, (b) Rectangular Prism, (c) Hemisphere

One of the distinct advantages of cellular materials is decreased weight. The final parts produced by this method demonstrate this potential reduction clearly. The cubic piece, for example, is nominally 8 cubic inches in volume, if the cubic space were entirely filled and there were no plates on either side of the truss section. With the designed mesostructure, the part volume is decreased to 2.77 cubic inches, only 35% of the initial volume. At a density of 2.67 grams per cm^3 for the A356 alloy, the truss part would only have a mass of approximately 121.2 grams. The final cast cubic part has an experimental mass of 170.3g, which includes the additional mass caused by the plates on top and bottom of the part.

From an initial evaluation, both the hemispherical and cubic pieces appear to fill properly with no missing trusses. The rectangular prism, on the other hand, is prone to unfilled trusses, specifically near the bottom of the piece. In addition to missing trusses, the bottom plate of the piece is hollow, rather than a completely filled plate of metal. Both of these phenomena can be seen in Figure 8, a cross-sectional view of one of the rectangular pieces. Likely causes for both aspects are trapped gasses occurring within the mold while the metal is being poured, thus preventing the bottom section from filling properly. By further adjusting the speed of metal flow, as well as adding additional venting holes on the sides of the exterior mold, these issues can be likely be avoided.

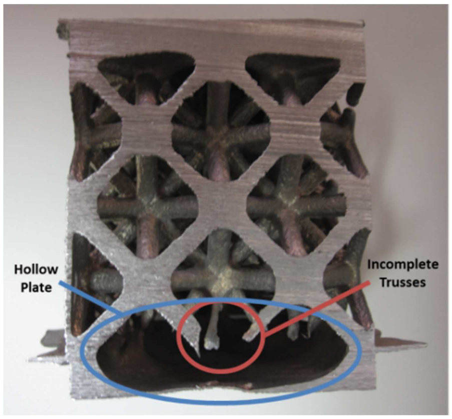

Figure 8. Visible Defects in Rectangular Part Quality

In addition to several unfilled trusses, this piece also demonstrates potential issues arising regarding consistent truss diameter. To investigate any significant issues with diameter consistency, 24 of the interior struts from the one of the cubic pieces (Figure 7a) were measured, as seen in Figure 9. The diameters for these 24 samples had an average value of 3.7 mm with a standard deviation of 0.2 mm. The range of the dataset was 0.9 mm, with the largest truss 13.5% larger than the average and the smallest truss 10.8% lower than the average. The average value of these struts is 27% smaller than the designed truss diameter (5.08mm), which is caused by metal shrinkage that is typical during metal casting.

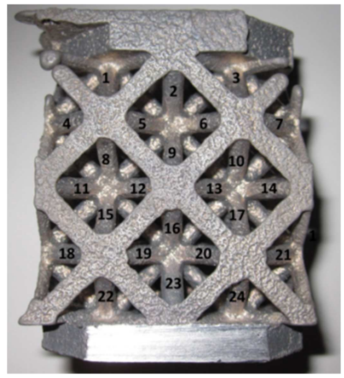

Figure 9. Measured Trusses for Diameter Evaluation

The authors briefly investigated variation of truss diameter between sections of the part as well, to determine if the struts at the top of the part were significantly different from those at the bottom. The specimen was divided into a top section (struts 1-7), a middle section (struts 8-17), and a bottom section (struts 18-24). The implementation of a one-way ANOVA analysis identified no significant difference between the diameters in the three sections. In fact, in this sample, all of the sections have the same average and standard deviation values of 3.7 mm and 0.2 mm respectively, precise to one decimal place.

To better determine the quality of the metal pour, the other half of the rectangular part from Figure 8 was ground flat and finely polished. This allows for the porosity of the final part to be observed through a stereo microscope. As Figure 10 shows, there are numerous porous defects (roughly 0.1 mm in diameter) present within the casting. To address this porosity, future experiments will focus in pouring the metal in an inert, vacuum environment.

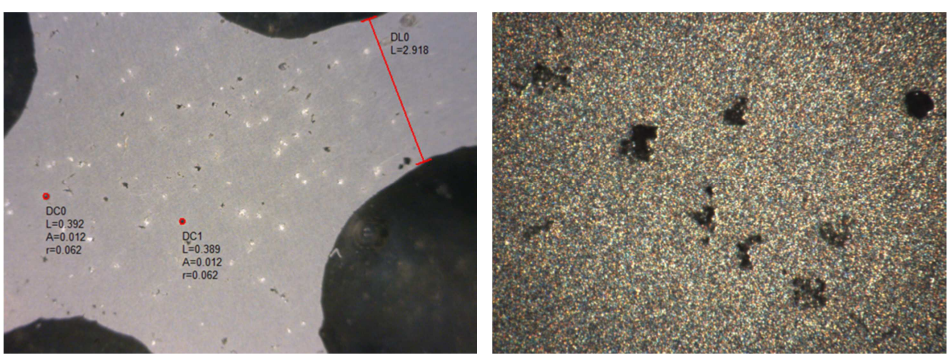

Figure 10. General Porosity with units in mm (left) and Detailed Porous Defects (right)

4.2. Mechanical Properties of Final Part

To provide a preliminary evaluation of the mechanical properties of the final part, a compression test was performed on a cast part (Figure 7a) that had no incomplete or missing trusses and little to no flash. The part was compressed at a rate of 1.5mm per second. A plot relating the crosshead displacement with the resultant load on the part is shown in Figure 11, along with an image of the final compressed specimen.

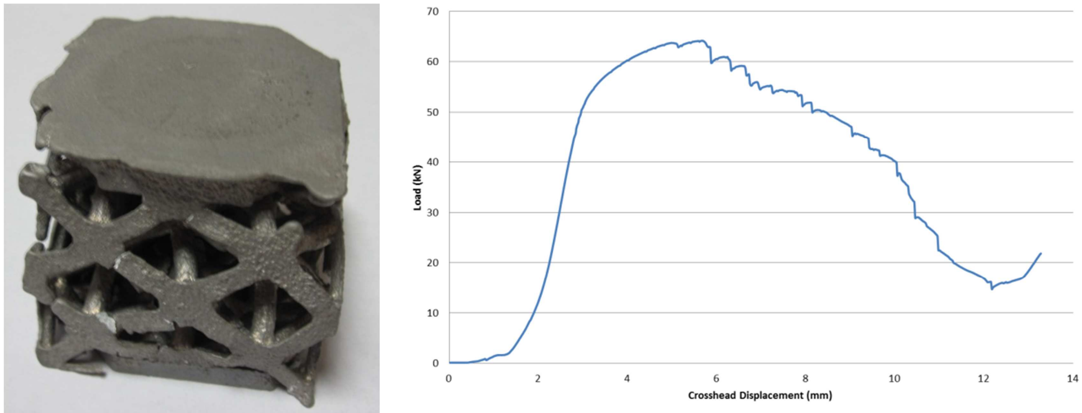

Figure 11. Crushed Specimen (left) and Load vs. Displacement Plot (right)

The compression test shows that the piece can withstand a maximum load of 64.09 kN before trusses within the part begin to fail. At approximately 12 mm displacement, the failed trusses began to impact each other within the part, causing the measured load to begin rising again. Further experimentation will seek to correlate the above experimental results with theoretical predictions of failure for an octet truss arrangement.

5. CONCLUSIONS AND RECOMMENDATIONS FOR FUTURE WORK

In this paper, a method for the creation of lightweight, metal cellular structures was presented utilizing the capabilities of indirect 3D printing and traditional casting techniques. Indirect 3D printing is advantageous in that it is scalable and relatively inexpensive, and the casting sand powders used for printing allow processing of many different alloys. The resulting part quality, while partially dependent on part geometry, demonstrates that this method is capable of producing completely filled truss structures with minimal diameter variation, In addition, experimentation shows that the octet structure within a cubic geometry is capable of supporting a 60 kN compressive force before truss failure begins.

For future work, efforts will be focused on combining topology optimization with the process described herein. Using topology optimization during the initial digital mold creation phase will allow for structures that are tailored to perform optimally under certain loading conditions. In addition, efforts will be undertaken to analytically model the flow of the molten metal through the mold, ensuring that the final parts are poured at to be completely filled, regardless of geometry. Finally, research will investigate the vacuum casting approaches to eliminate porosity.

6. ACKNOWLEDGMENTS

The authors would like to thank Dr. Carlos Suchicital for his assistance and insight regarding the molding and casting processes. The authors also acknowledge John Lohr, undergraduate researcher for the DREAMS Lab, for his assistance with part printing and experimentation.

7. REFERENCES

1. Banhart, J. and D. Weaire, 2002, "On the Road Again: Metal Foams Find Favor," *Physics Today*, July, pp. 37-42.
2. Banhart, J., 2000, "Manufacturing Routes for Metallic Foams," *The Member Journal of the Minerals, Metals & Materials Society*, Vol. 52, No. 12, pp. 22-27.
3. Evans, A. G., J. W. Hutchinson and M. F. Ashby, 1999, "Multifunctionality of Cellular Metal Systems," *Progress in Material Science*, Vol. 43, pp. 171-121.
4. Evans, A. G., J. W. Hutchinson, N. A. Fleck, M. F. Ashby and H. N. G. Wadley, 2001, "The Topological Design of Multifunctional Cellular Metals," *Progress in Material Science*, Vol. 46, pp. 309-327.
5. Seepersad, C. C., R. S. Kumar, J. K. Allen, F. M. Mistree and D. L. McDowell, 2004, "Multifunctional Design of Prismatic Cellular Materials," *Journal of Computer-Aided Materials Design*, Vol. 11, No 2, pp. 163-181.
6. Seepersad, C. C., J. K. Allen, D. McDowell and F. M. Mistree, 2006, "Robust Design of Cellular Materials with Topological and Dimensional Imperfections," *Journal of Mechanical Design*, Vol. 128, No. 6, pp. 1285-1297.
7. Thompson, S. C., H. Muchnick, H. Choi, D. McDowell, J. K. Allen and F. M. Mistree, 2006, "Robust Materials Design of Blast Resistant Panels," *AIAA/ISSMO Multidisciplinary Analysis and Optimization Conference*, Portsmouth, VA, AIAA 2006-7005.
8. Ashby, M. F., A. G. Evans, N. A. Fleck, L. J. Gibson, J. W. Hutchinson and H. N. G. Wadley, 2000, *Metal Foams: A Design Guide*, Butterworth-Heinemann, Woburn, MA.
9. Gibson, L. J. and M. F. Ashby, 1997, *Cellular Solids: Structures and Properties*, Cambridge University Press, Cambridge, UK..
10. Wadley, H. N. G., N. A. Fleck and A. Evans, 2003, "Fabrication and Structural Performance of Periodic Cellular Metal Sandwich Structures," *Composites Science and Technology*, Vol. 63, pp. 2331-2343.
11. Mori, L. F., S. Lee, Z. Y. Xue, A. Vaziri, D. T. Queheillalt, K. P. Dharmasena, H. N. G. Wadley, J. W. Hutchinson and H. D. Espinosa, 2007, “ Deformation and fracture modes of sandwich structures subjected to underwater impulsive loads,” *Journal of Mechanics of Materials and Structures*. Vol. 2, No. 10.
12. Queheillalt, D.T., Y. Murty, and H. N. G. Wadley, 2008, “Mechanical properties of an extruded pyramidal lattice truss sandwich structure,” *Scripta Materialia*, Vol. 58, pp. 76-79.

13. Queheillalt, D.T., V. S. Deshpande, and H. N. G. Wadley, 2007, “Truss waviness effects in cellular lattice structures,” *Journal of Mechanics of Materials and Structures*, Vol. 2, No. 9.

14. Moongkhamklang, P. and H. N. G. Wadley, 2010, “Titanium alloy lattice structures with millimeter scale cell sizes,” *Advanced Engineering Materials*, Vol. 12, No. 11, pp. 1111-1116.

15. Sypeck, D. J. and H. N. G. Wadley, 2002, "Cellular Metal Truss Core Sandwich Structures," *Advanced Engineering Materials*, Vol. 4, No. 10, pp. 759-764.

16. Pham, D. T., S. S. Dimov, C. Ji and R. S. Gault, 2003, "Layer Manufacturing Processes: Technology Advances and Research Challenges," *1st International Conference on Advanced Research in Virtual and Rapid Prototyping*, Leiria, Portugal, pp. 107-113.

17. Brooks, W., C. Sutcliffe, W. Cantwell, P. Fox, J. Todd and R. Mines, 2005, "Rapid Design and Manufacture of Ultralight Cellular Materials," *International Solid Freeform Fabrication Symposium*, Austin, TX., pp. 231-241.

18. Cansizoglu, O., D. Cormier, O. Harrysson, H. West and T. Mahale, 2006, "An Evaluation of Non-Stochastic Lattice Structures Fabricated Via Electron Beam Melting," *International Solid Freeform Fabrication Symposium*, Austin, TX., pp. 209-2119.

19. Yang, L., O. Harrysson, H. West II and D. Cormier, 2011, “Design and characterization of orthotropic re-entrant auxetic structures made via EBM using Ti6Al4v and pure copper,” *International Solid Freeform Fabrication Symposium*, Austin TX.

20. Agarwala, M., D. Bourell, J. Beaman, H. Marcus and J. Barlow, 1995, "Direct Selective Laser Sintering of Metals," *Rapid Prototyping Journal*, Vol. 1, No. 1, pp. 26-36.

21. Williams, C. B., F. Mistree and D. W. Rosen, 2005, “Investigation of Solid Freeform Fabrication Processes for the Manufacture of Parts with Designed Mesostructure,” *ASME IDETC Design for Manufacturing and the Life Cycle Conference*. Long Beach, California

22. Zaeh, M. and Branner G., 2010, “Investigations on residual stresses and deformations in selective laser melting,” *Production Engineering*, Vol. 4, No. 1, pp. 35-45.

23. Shiomi, M., K. Osakada, et al, 2004, “Residual Stress within metallic model made by selective laser melting process” *CIRP Annals – Manufacturing Technology*, Vol. 53, No. 1, pp. 195-198.

24. Mumtaz, K., P. Vora, and N. Hopkinson, 2011, “A Method to Eliminate Anchors/Supports from Directly Laser Melted Metal Powder Bed Processes,” *International Solid Freeform Fabrication Symposium*, Austin TX.

25. Jamcorp Inc., 2004, "Jonathon Aerospace Materials Website," <www.jamcorp.com> (Unavailable).

26. Nathal, M. V., J. D. Whittenberger, M. G. Hebsur, P. T. Kantzos, and D. L. Krause, 2004 “Superalloy Lattice Block Structures,” NASA/TM-2004-213109, *10th International Symposium on Superalloys*, September 19- 23, Champion, PA.

27. Wadley, H. N. G., N. A. Fleck and A. Evans, 2003, "Fabrication and Structural Performance of Periodic Cellular Metal Sandwich Structures," *Composites Science and Technology*, Vol. 63, pp. 2331-2343.

28. Hattiangadi, A. and A. Bandyopadhyay, 1999, "Processing, Characterization and Modeling of Non-Random Porous Ceramic Structures," *International Solid Freeform Fabrication Symposium*, Austin, TX, pp. 319-326.

29. Chiras, S., D. R. Mumm, A. G. Evans, N. Wicks, J. W. Hutchinson, K. Dharmasena, H. N. G. Wadley and S. Fichter, 2002, "The Structural Performance of Near-Optimized Truss Core Panels," *International Journal of Solids and Structures,* Vol. 39, pp. 4093-4115.

30. Lyons, A., S. Krishnan, J. Mullins, M. Hodes and D. Hernon, 2009, "Advanced Heat Sinks Enabled by Three-Dimensional Printing," *International Solid Freeform Fabrication Symposium*, Austin, TX.

31. 3D Systems, 2012, "Solutions: Metal Casting," <http://www.zcorp.com/en/Solutions/Castings--Patterns--Molds/spage.aspx>.

32. ExOne, 2012, "S-Print: Improved Productivity in a Compact Design," <http://exone.com/materialization/systems/S-Print>.

33. voxeljet, 2012, "Large-format sand moulds for metal casting," <http://www.voxeljet.de/fileadmin/Voxeljet/Services/Sand_casting_2012.pdf>.

34. Chhabra, M., and R. Singh, 2011, "Rapid casting solutions: A review," *Rapid Prototyping Journal,* Vol. 17, No. 5, pp. 328-350.

35. Stankiewicz, M., G. Budzik, M. Patrzalek, M. Wieczorowski, M. Grzelka, H. Matysiak, and J. Slota, 2010, "The scope of application of incremental rapid prototyping methods in foundry engineering," *Archives of Foundry Engineering*, Vol 10, Special Issue 1, pp. 405-410.

36. Bassoli, E., and E. Atzeni, 2009, "Direct metal rapid casting: mechanical optimization and tolerance calculation", *Rapid Prototyping Journal*, Vol. 15, No. 4, pp. 238 – 243.

37. McKenna, N., S. Singamneni, O. Diegel, D. Singh, T. Neitzert, J. St. George, A. R. Choudhury, and P. Yarlagadda, 2008, "Metal casting through 3d printing: A critical analysis of the mould characteristics," *9th Global Congress on Manufacturing and Management*, November 12-14, Surfers Paradise, Australia.

38. Gill, S. S., and M. Kaplas, 2011, "Efficacy of Powder-based three-dimensional printing (3DP) technologies for rapid casting of light alloys," *International Journal of Advance Manufacturing Technology*, Vol. 52, pp. 53-64.

39. Gill, S.S., and M. Kaplas, "Comparative Study of 3D Printing Technologies for Rapid Casting of Aluminum Alloy," *Materials and Manufacturing Processes,* Vol. 24, No. 12, pp. 1405-1411.

40. Chhabra, M., and R. Singh, 2012, "Obtaining desired surface roughness of castings produced using ZCast direct metal casting process through Taguchi's experimental approach", *Rapid Prototyping Journal*, Vol. 18, No. 6.

41. Bassoli, E., A. Gatto, L. Iuliano, and M. G. Violante, 2007, "3D printing technique applied to rapid casting", *Rapid Prototyping Journal*, Vol. 13, No. 3, pp.148 – 155.

42. Budzik, G., "Possibilities of utilizing 3dp technology for foundry mould making," *Archives of Foundry Engineering*," Vol. 7, No. 2, pp. 65-68.

43. Kawola, J., “ZCast Direct Metal Casting: From Data to Cast Aluminum in 12 hours,” Z Corporation, <http://www.3dprint.no/images/Nyheter_info/ZCast%20info.pdf>.

44. Williams, C.B., F. Mistree, and D. W. Rosen, 2005, “Towards the Design of a Layer-Based Additive Manufacturing Process for the Realization of Metal Parts of Designed Mesostructures,” *International Solid Freeform Fabrication Symposium*, August 1-3, Austin, TX, pp. 217-230.

45. netFabb, 2011, “Selective Space Structures (3S) – your tool for creation of complex structures,” <http://netfabb.com/structure.php>.